

A Realization of Real-time Sequence Generator for k -th Powers of Natural Numbers by
One-Dimensional Cellular Automata

Naoki KAMIKAWA

Institute of Informatics, Univ. of Osaka Electro-Communication,
18-8 Hatsu-cho, Neyagawa-shi, Osaka, 572-8530, Japan

Hiroshi UMEO

Univ. of Osaka Electro-Communication,
18-8 Hatsu-cho, Neyagawa-shi, Osaka, 572-8530, Japan

Received: February 15, 2020

Revised: May 5, 2020

Accepted: May 15, 2020

Communicated by Sayaka Kamei

Abstract

A cellular automaton (CA) is a well-studied non-linear computational model of complex systems in which an infinite one-dimensional array of finite state machines (cells) updates itself in a synchronous manner according to a uniform local rule. A sequence generation problem on the CA model has been studied for a long time and a lot of generation algorithms has been proposed for a variety of non-regular sequences such as $\{2^n \mid n = 1, 2, 3, \dots\}$, primes, Fibonacci sequences etc. In this paper, we study a real-time sequence generation algorithm for k -th powers of natural numbers on a CA. In the previous studies, Kamikawa and Umeo (2012, 2019) showed that sequences $\{n^2 \mid n = 1, 2, 3, \dots\}$, $\{n^3 \mid n = 1, 2, 3, \dots\}$ and $\{n^4 \mid n = 1, 2, 3, \dots\}$ can be generated in real-time by one-dimensional CAs. We extend the generation algorithm for $\{n^4 \mid n = 1, 2, 3, \dots\}$ shown by Kamikawa and Umeo, and present a generation algorithm for the sequence $\{n^k \mid n = 1, 2, 3, \dots\}$ implemented.

Keywords: Cellular automata, Real-time sequence generation problem, Parallel algorithm, Computational complexity

1 Introduction

A model of cellular automaton (CA) was originally devised for studying self-reproduction in biological systems by J. von Neumann [11]. Thereafter, the cellular automaton has been studied in many fields such as complex systems, computability theory, mathematics, and theoretical biology.

A sequence generation problem is one of the major topics in the application of CAs. Arisawa [1], Fischer [2], Korec [10], and Kamikawa and Umeo [3, 4, 5, 6, 7, 8, 9] studied the sequence generation problem, where the leftmost cell of the array generates an infinite non-regular sequence indicated by an internal state set. In those studies, much attention has been paid to the developments of real-time generation algorithms and their small-state implementations on CAs for specific non-regular sequences.

Here we study a real-time sequence generation algorithm for k -th powers of natural numbers that is $\{n^k | n = 1, 2, 3, \dots\}$, $k \geq 2$. In the previous studies, Kamikawa and Umeo [6], [8], [9] showed that sequences $\{n^2 | n = 1, 2, 3, \dots\}$, $\{n^3 | n = 1, 2, 3, \dots\}$ and $\{n^4 | n = 1, 2, 3, \dots\}$ can be generated in real-time by one-dimensional CAs. In this paper, we extend the generation algorithm for $\{n^4 | n = 1, 2, 3, \dots\}$ shown by Kamikawa and Umeo [9], and present a generation algorithm for the sequence $\{n^k | n = 1, 2, 3, \dots\}$ implemented. The sequence $\{n^k | n = 1, 2, 3, \dots\}$ generation algorithm when $k=2, 3$ requires more internal state than generation algorithms shown by Kamikawa and Umeo [6], [8]. Nevertheless, we consider that the algorithm is worth in that sequence $\{n^k | n = 1, 2, 3, \dots\}$ can be generated in real-time for any k , $k \geq 2$.

Our motivation to study the sequence generation problem on CAs is to want to show computing power of CAs. Also, it is known that primes, Fibonacci sequences, and so on appear in various natural phenomena. For example, the Fibonacci sequence appears in biological modelings such as the number of petals in a flower, branching in trees, and the family tree of honeybees. Our sequence generation algorithms would be useful in the simulation and modeling biological pattern formations using CAs.

2 Sequence Generation Problem

A cellular automaton consists of a semi-infinite array of identical finite state automaton, each located at a positive integer point (See Figure 1).

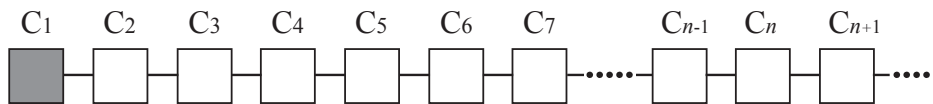


Figure 1: One-dimensional cellular automaton.

Each automaton is referred to as a cell. A cell at point i is denoted by C_i , where $i \geq 1$. Each C_i , except for C_1 , is connected to its left- and right-neighbor cells via a communication link. Each cell can know a state of its left- and right-neighbor cells via the communication link. One distinguished leftmost cell C_1 , the communication cell, is connected to outside and C_2 .

Formally, a cellular automaton (abbreviated by CA) consists of a semi-infinite array of finite state automaton $M = (Q, \delta, \mathbf{b}, \mathbf{a})$, where

1. Q is a finite set of internal states.
2. δ is a transition function defining the next state of a cell such that $\delta: Q \times Q \times Q \rightarrow Q$, where $\delta(\mathbf{w}, \mathbf{x}, \mathbf{y}) = \mathbf{z}$ ($\mathbf{w}, \mathbf{x}, \mathbf{y}, \mathbf{z} \in Q$) has the following meaning: Let t be an integer such that $t \geq 0$. We assume that at step t the cell C_i ($i \geq 2$) is in state \mathbf{x} , the left cell C_{i-1} is in state \mathbf{w} and the right cell C_{i+1} is in state \mathbf{y} . Then, at the next step $t + 1$, C_i takes state \mathbf{z} . The leftmost cell C_1 always gets a special state $\$$ from its outside as the state of its left cell. A quiescent state $\mathbf{q} \in Q$ has a property such that $\delta(\mathbf{q}, \mathbf{q}, \mathbf{q}) = \mathbf{q}$ and $\delta(\$, \mathbf{q}, \mathbf{q}) = \mathbf{q}$.
3. A state \mathbf{b} is a special state in Q which C_1 takes at the initial configuration.
4. A state \mathbf{a} is a special state in Q to specify a designated state of C_1 in the definition of sequence generation.

Here we introduce some notations. A transition rule $\delta(w, x, y) = z$ is simply expressed as $\mathbf{w} \ \mathbf{x} \ \mathbf{y} \rightarrow \mathbf{z}$. To denote a configuration on a cellular array of length n at time t , we use the following convention: $t : \mathbf{S}_1^t \dots \mathbf{S}_n^t$, where \mathbf{S}_i^t denotes the state of the i th cell C_i at time t , $1 \leq i \leq n, t \geq 0$.

For convenience, a notation $t : \overbrace{\mathbf{S} \dots \mathbf{S}}^{[i,j]}$ is also used to denote a partial configuration on neighboring $j - i + 1$ cells, starting from the i th cell C_i to C_j , all in state \mathbf{S} at time t .

We define a new symbol \Rightarrow that shows a synchronous updating of one configuration to the next one with simultaneous applications of the transition rule to each cell. For example, a one-step state transition of M is shown as follows:

$$t : \overbrace{S_1^t \dots S_n^t}^{[1,n]} \Rightarrow t + 1 : \overbrace{S_1^{t+1} \dots S_n^{t+1}}^{[1,n]}.$$

We now define the sequence generation problem on CA. Let M be a CA, j be a natural number such that $j \geq 1$, and $\{t_n \mid n = 1, 2, 3, \dots\}$ be an infinite monotonically increasing positive integer sequence defined on natural numbers such that $t_n \geq n$ for any $n \geq 1$. We have a semi-infinite array of cells, shown in Figure 1, and all cells, except for C_1 , are in a quiescent state q at time $t = 0$. The communication cell C_1 takes a special state b in Q at time $t = 0$ for initiation of the sequence generator. We say that M generates a sequence $\{t_n \mid n = 1, 2, 3, \dots\}$ in j -linear-time if and only if the leftmost end cell of M falls into a special state a in Q at time $t = j \cdot t_n$. Note that M generates the n th term of t_n at time $t = j \cdot t_n$. In particular, when $j = 1$, we call M a real-time sequence generator. In this case, M generates a sequence $\{t_n \mid n = 1, 2, 3, \dots\}$ without any time delay. Therefore, when $j = 1$, M is optimal in generation steps.

3 Real-time sequence generation algorithm for k -th powers of natural numbers

Let k be a natural number such that $k \geq 2$. In this section, we show a implementation of real-time sequence generation algorithm for $\{n^k \mid n = 1, 2, 3, \dots\}$. This algorithm consists of $\{n^2 \mid n = 1, 2, 3, \dots\}$, $\{n^3 \mid n = 1, 2, 3, \dots\}$, \dots , $\{n^{k-2} \mid n = 1, 2, 3, \dots\}$ and $\{n^{k-1} \mid n = 1, 2, 3, \dots\}$ generation algorithms. At first, we indicate a design of real-time generation algorithm using generation algorithm for $\{n^2 \mid n = 1, 2, 3, \dots\}$ as an example.

3.1 Real-time sequence generation algorithm for $\{n^2 \mid n = 1, 2, 3, \dots\}$

Let i be a natural number such that $i \geq 1$, a_i be an infinite monotonically increasing positive integer sequence defined on natural numbers such that $a_1 = 1, a_2 = 4, a_3 = 9, \dots, a_i = i^2$, b_i be a difference sequence of a_i such that $b_i = 2i + 1$. Thus, when the communication cell C_1 takes a special state a at time $t = a_i$, C_1 falls into a special state a at time $t = a_i + b_i = a_{i+1}$.

3.1.1 Space-Time Diagram

We give a sketch of the real-time sequence generation algorithm for $\{n^2 \mid n = 1, 2, 3, \dots\}$. This algorithm is described in terms of three signals which propagate at various speeds in the cellular space. We call them waves. They are a -wave, b -wave and c -wave, respectively. See Figure 2 that illustrates a space-time diagram for the real-time generation of the sequence. The propagation speed and direction of each wave in a space-time domain is as follows:

- a -wave: 1/1-speed, right,
- b -wave: 1/1-speed, left, and
- c -wave: 0-speed, stationary (marker).

A rough sketch of the sequence $\{n^2 \mid n = 1, 2, 3, \dots\}$ generation algorithm is as follows:

1. At the time $t = 1$, the leftmost cell C_1 falls into a special state a , the a -wave is generated, the c -wave is generated by the cell C_2 , and the c -wave keeps a marker

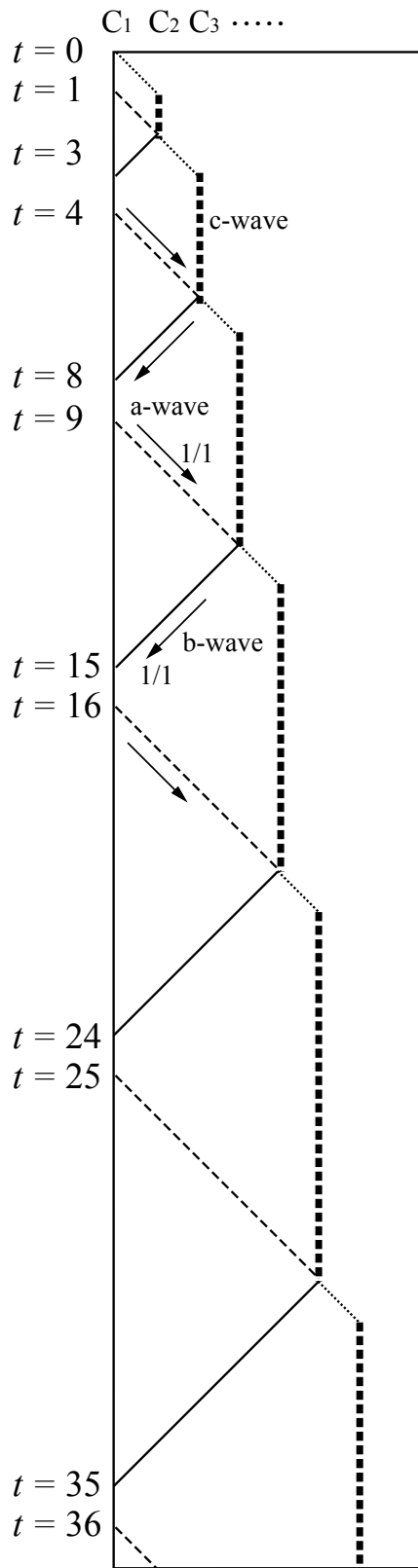


Figure 2: Space-time diagram for real-time generation of sequence $\{n^2 | n = 1, 2, 3, \dots\}$.

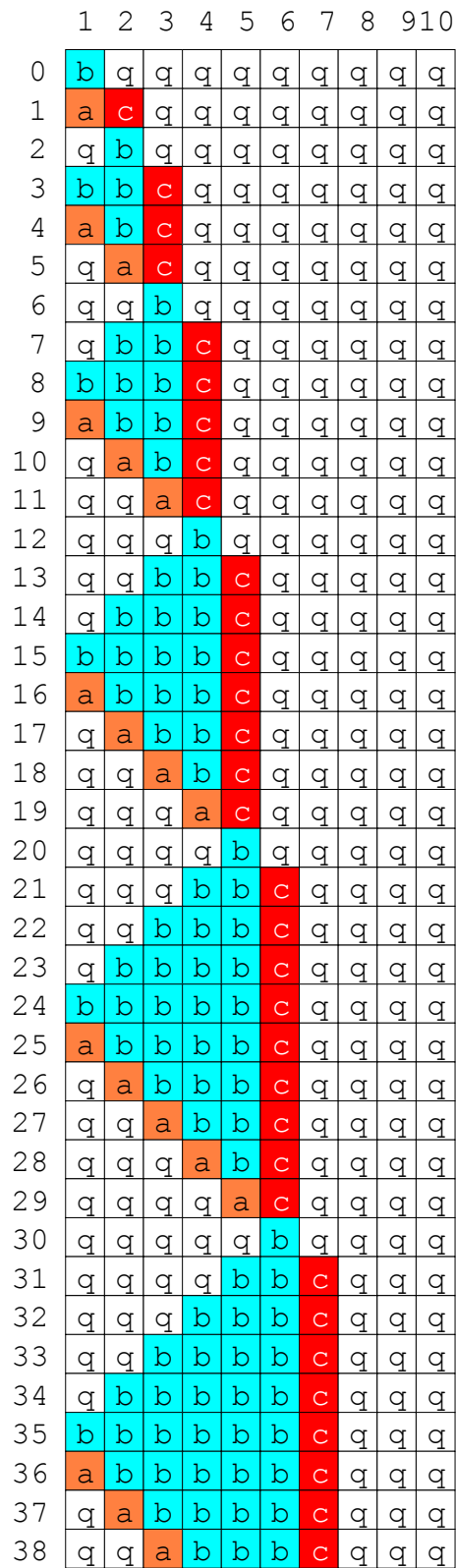


Figure 3: A configuration of real-time generation of sequence $\{n^2 | n = 1, 2, 3, \dots\}$.

2. The a-wave propagates in the right direction towards the c-wave at 1/1 speed, and collides with the c-wave at time $t = 2$. Then the a-wave is eliminated, the c-wave moves to the right cell, and the b-wave propagated in left direction at 1/1 speed is generated. The c-wave keeps a marker. At the arrival of the b-wave at the leftmost cell C_1 , the b-wave is deleted. At time $t = 4$ one step later, the leftmost cell C_1 falls into a special state **a**, and the a-wave is generated.
3. Let j be any natural number such that $j \geq 2$. At time $t = a_j$, the c-wave exists on the cell C_{j+1} , the cell C_1 falls into the special state **a**, and the a-wave is generated. The a-wave propagates in right direction at 1/1 speed, so the a-wave hits the c-wave at time $t = a_j + j$. Then the c-wave moves to the right cell C_{j+2} , and the b-wave propagated in left direction at 1/1 speed is generated. The b-wave reaches the leftmost cell C_1 at time at time $t = a_j + j + j$, and the b-wave is deleted. At time $t = a_j + 2j + 1 = a_j + b_j = a_{j+1}$ one step later, the a-wave is generated, and the cell C_1 falls into the special state **a**.

Propagations of a-, b-, and c-waves on the space-time diagram shown in Figure 2 is the same as those of the generation algorithm shown by Kamikawa and Umeo [6], but waves implementation is different.

3.1.2 Implementation

A four-state real-time sequence generator for $\{n^2 \mid n = 1, 2, 3, \dots\}$ consists of a semi-infinite array of finite state automaton $M = (Q, \delta, \mathbf{b}, \mathbf{a})$, where $Q = \{\mathbf{q}, \mathbf{a}, \mathbf{b}, \mathbf{c}\}$. The state **c** is increasing from the sequence $\{n^2 \mid n = 1, 2, 3, \dots\}$ generation algorithm show by Kamikawa and Umeo [6]. Table 1 is the transition function \mathcal{R}_{n^2} for the real-time sequence $\{n^2 \mid n = 1, 2, 3, \dots\}$ generator.

Table 1: A four-state transition function \mathcal{R}_{n^2} for real-time generation of sequence $\{n^2 \mid n = 1, 2, 3, \dots\}$.

q		Right State			
		q	a	b	c
Left State	q	q	q	b	
	a				
	b	c			
	c	q			
	\$	q	q	b	

a		Right State			
		q	a	b	c
Left State	q			q	q
	a				
	b				
	c				
	\$			q	b

b		Right State			
		q	a	b	c
Left State	q	b		b	
	a			a	a
	b			b	b
	c				
	\$	a		a	

c		Right State			
		q	a	b	c
Left State	q				
	a	b			
	b	c			
	c				
	\$				

The initial configuration of M at time $t = 0$ is:

$$t = 0 : \underbrace{\mathbf{b}}^{[1]} \underbrace{\mathbf{q}, \dots, \mathbf{q}}^{[2, \dots]}$$

At time $t = 1$, all cells, except for C_1 and C_2 , keep the quiescent state **q** with the rule $\mathbf{q} \mathbf{q} \mathbf{q} \rightarrow \mathbf{q}$. C_1 and C_2 fall into the states **a** and **c** with the rules $\mathbf{\$} \mathbf{b} \mathbf{q} \rightarrow \mathbf{a}$ and $\mathbf{b} \mathbf{q} \mathbf{q} \rightarrow \mathbf{c}$ in \mathcal{R}_{n^2} , respectively. The configuration at time $t = 1$ is:

$$t = 1 : \underbrace{\mathbf{a}}^{[1]} \underbrace{\mathbf{c}}^{[2]} \underbrace{\mathbf{q}, \dots, \mathbf{q}}^{[3, \dots]}$$

At time $t = 2$, all cells, except for C_1 , C_2 and C_3 , keep the quiescent state **q** with the rule $\mathbf{q} \mathbf{q} \mathbf{q} \rightarrow \mathbf{q}$. C_1 , C_2 and C_3 fall into the state **q**, **b** and **q** with the rules $\mathbf{\$} \mathbf{a} \mathbf{c} \rightarrow \mathbf{q}$, $\mathbf{a} \mathbf{c} \mathbf{q} \rightarrow \mathbf{b}$ and $\mathbf{c} \mathbf{q} \mathbf{q} \rightarrow \mathbf{q}$ in \mathcal{R}_{n^2} , respectively. The configuration at time $t = 2$ is:

$$t = 2 : \underbrace{\mathbf{q}}^{[1]} \underbrace{\mathbf{b}}^{[2]} \underbrace{\mathbf{q}, \dots, \mathbf{q}}^{[3, \dots]}$$

In this way, M takes the following configurations at time $t = 0 \sim 9$.

$$\begin{array}{l}
 t = 0 : \quad \underbrace{\text{b}}_{[1]} \quad \underbrace{\text{q}, \dots, \text{q}}_{[2, \dots]} \Rightarrow \\
 t = 1 : \quad \underbrace{\text{a}}_{[1]} \quad \underbrace{\text{c}}_{[2]} \quad \underbrace{\text{q}, \dots, \text{q}}_{[3, \dots]} \Rightarrow \\
 t = 2 : \quad \underbrace{\text{q}}_{[1]} \quad \underbrace{\text{b}}_{[2]} \quad \underbrace{\text{q}, \dots, \text{q}}_{[3, \dots]} \Rightarrow \\
 t = 3 : \quad \underbrace{\text{bb}}_{[1,2]} \quad \underbrace{\text{c}}_{[3]} \quad \underbrace{\text{q}, \dots, \text{q}}_{[4, \dots]} \Rightarrow \\
 t = 4 : \quad \underbrace{\text{a}}_{[1]} \quad \underbrace{\text{b}}_{[2]} \quad \underbrace{\text{c}}_{[3]} \quad \underbrace{\text{q}, \dots, \text{q}}_{[4, \dots]} \Rightarrow \\
 t = 5 : \quad \underbrace{\text{q}}_{[1]} \quad \underbrace{\text{a}}_{[2]} \quad \underbrace{\text{c}}_{[3]} \quad \underbrace{\text{q}, \dots, \text{q}}_{[4, \dots]} \Rightarrow \\
 t = 6 : \quad \underbrace{\text{qq}}_{[1,2]} \quad \underbrace{\text{b}}_{[3]} \quad \underbrace{\text{q}, \dots, \text{q}}_{[4, \dots]} \Rightarrow \\
 t = 7 : \quad \underbrace{\text{q}}_{[1]} \quad \underbrace{\text{bb}}_{[2,3]} \quad \underbrace{\text{c}}_{[4]} \quad \underbrace{\text{q}, \dots, \text{q}}_{[5, \dots]} \Rightarrow \\
 t = 8 : \quad \underbrace{\text{b}, \dots, \text{b}}_{[1, \dots, 3]} \quad \underbrace{\text{c}}_{[4]} \quad \underbrace{\text{q}, \dots, \text{q}}_{[5, \dots]} \Rightarrow \\
 t = 9 : \quad \underbrace{\text{a}}_{[1]} \quad \underbrace{\text{bb}}_{[2,3]} \quad \underbrace{\text{c}}_{[4]} \quad \underbrace{\text{q}, \dots, \text{q}}_{[5, \dots]}
 \end{array}$$

The overview of the wave generation and its implementation in terms of four states is as follows:

- **a-wave:** The a-wave is depicted by the state **a**. It is generated on C_1 . The a-wave propagates in the right direction at 1/1-speed and meets the c-wave which is a stationary state staying on a cell. When the a-wave hits the c-wave, the b-wave which return to the left direction are generated. See Figure 2.
- **b-wave:** The b-wave is depicted by the state **b**. The b-wave propagates in the left direction at 1/1-speed and hits the cell C_1 . When the b-wave collides with the cell C_1 , the a-wave which returns to the right direction is generated.
- **c-wave:** The c-wave is represented by the state **c**. The c-wave acts as a marker. When the a-wave hits the c-wave, the b-wave which returns to the left direction is generated, the c-wave moves to the right cell. In the sequence $\{n^2 \mid n = 1, 2, 3, \dots\}$ generation algorithm shown by Kamikawa and Umeo [6], a- and c-waves are represented by the state **a**. Because of the generation when $k \geq 3$, this algorithm expresses a- and c-waves by state **a** and **c**, respectively.

We have implemented the rule set in Table 1 on a computer. In Figure 3, we show a number of configurations in the space-time domain such that $C_\ell, 1 \leq \ell \leq 10, 0 \leq t \leq 38$.

3.2 A implementation of real-time sequence generation algorithm for $\{n^3 \mid n = 1, 2, 3, \dots\}$

In this section, we show a real-time generation algorithm for $\{n^3 \mid n = 1, 2, 3, \dots\}$ designed using sequence $\{n^2 \mid n = 1, 2, 3, \dots\}$ generation process. The space-time diagram of this algorithm is

different from that of two algorithms shown by Kamikawa and Umeo [8]. This algorithm is made by extending the method of sequence $\{n^4 \mid n = 1, 2, 3, \dots\}$ generation algorithm shown by Kamikawa and Umeo [9], and contains the real-time sequence generation algorithm for $\{n^2 \mid n = 1, 2, 3, \dots\}$ shown in 3.1 inside. Let i be a natural number such that $i \geq 1$, c_i be an infinite monotonically increasing positive integer sequence defined on natural numbers such that $c_1 = 1, c_2 = 8, c_3 = 27, \dots, c_i = i^3$, d_i be a difference sequence of c_i such that $d_i = 3i^2 + 3i + 1$.

3.2.1 Space-Time Diagram

A real-time sequence generator for $\{n^3 \mid n = 1, 2, 3, \dots\}$ consists of a semi-infinite array of finite state automaton M . Table 2 is the transition function \mathcal{R}_{n^3} for the real-time sequence $\{n^3 \mid n = 1, 2, 3, \dots\}$ generator.

The initial configuration of M at time $t = 0$ is:

$$t = 0 : \underbrace{[1]}_{u_0} \underbrace{[2, \dots]}_{q, \dots, q}.$$

In Figure 4, we show a space-diagram for real-time generation of sequence $\{n^3 \mid n = 1, 2, 3, \dots\}$.

This algorithm uses six waves in addition to generation algorithm for $\{n^2 \mid n = 1, 2, 3, \dots\}$. They are *u-wave*, *x-wave*, *y-wave*, *z-wave*, *e-wave* and *f-wave*, respectively. Figure 5 shows snapshots of the generation processes from time $t = 0$ to $t = 8$. These configurations can be obtained by applying the rule set $\mathcal{R}_{n^3_1}$ given in Table 3 to the initial configuration.

Next we consider the generation processes at time $t \geq 8$. Let j be a natural number such that $j \geq 2$. At time $t = j^3$, M takes as follows:

$$t = j^3 : \underbrace{[1]}_{a} \underbrace{[2, \dots, j-1]}_{q, \dots, q} \underbrace{[j]}_{x3} \underbrace{[j+1, \dots]}_{q, \dots, q}.$$

The communication cell C_1 takes the special state a at time $t = c_j = j^3$. At the time $t = c_j + d_j = j^3 + 3j^2 + 3j + 1 = (j+1)^3$, the communication cell C_1 falls into the special state a by waves propagation according to the each term in the difference sequence of $d_j = 3j^2 + 3j + 1$. We consider the generation process when $j^3 \leq t \leq j^3 + 3j^2$, $j^3 + 3j^2 \leq t \leq j^3 + 3j^2 + 3j + 1$, respectively.

Case (I) $j^3 \leq t \leq j^3 + 3j^2$: At first, we show the generation process at $j^3 \leq t \leq j^3 + 3j^2$. In this process, M transitions $3j^2$ steps internally using the sequence generation algorithm for $\{n^2 \mid n = 1, 2, 3, \dots\}$. In Figure. 6, we show a space-time diagram at $j^3 \leq t \leq j^3 + 3j^2$.

The sequence generation algorithm for $\{n^2 \mid n = 1, 2, 3, \dots\}$ works between the leftmost cell C_1 and the x-wave. When the a-wave hits the x-wave, the y-wave is generated instead of the b-wave. Since the x-wave exists on the cell C_j , the y-wave reaches the leftmost cell C_1 at time $t = j^3 + j^2 - 1$. At the next step $t = j^3 + j^2$, the sequence generation algorithm for $\{n^2 \mid n = 1, 2, 3, \dots\}$ is restarted. This algorithm works three times between the leftmost cell C_1 and the x-wave. When the a-wave hits the x-wave for the third times, the x-wave moves to the cell C_{j+1} , the z-wave is generated instead of the y-wave. The z-wave propagates in left direction at 1/1 speed and hits the leftmost cell C_1 at time $t = j^3 + 3j^2 - 1$. At the next step $t = j^3 + 3j^2$, the next generation process is started.

Case (II) $j^3 + 3j^2 \leq t \leq j^3 + 3j^2 + 3j + 1$: In this case, the e-, f- and z-waves propagate for space-time diagram shown in Figure 7.

At time $t = j^3 + 3j^2$, the e-wave is generated, and propagates in right direction at 1/1 speed. The e-wave collides with the x-wave on the cell C_{j+1} at time $t = j^3 + 3j^2 + j$. Then the e-wave is deleted and the f-wave is generated. The f-wave propagates in left direction at 1/2 speed and hits the leftmost cell C_1 at time $t = j^3 + 3j^2 + 3j$. So, the f-wave is eliminated. At the next step $t = j^3 + 3j^2 + 3j + 1 = (j+1)^3$, the communication cell C_1 falls into the special state a . Then M takes as follows:

Table 2: A transition function \mathcal{R}_{n^3} for real-time generation of sequence $\{n^3 | n = 1, 2, 3, \dots\}$.

q State	59: \$ q u7 → a	e State	x2 State
1: q q q → q	60: \$ q x4 → e	106: q e q → q	128: q x2 q → x3
2: q q a2 → q	61: \$ q x6 → e	107: q e x5 → q	x3 State
3: q q b → b	62: \$ q x8 → b	108: q e x7 → q	129: q x3 q → x3
4: q q e → e	a State	109: \$ e q → b	130: a x3 q → x3
5: q q f1 → q	63: \$ a q → a2	110: \$ e x5 → b	131: a2 x3 q → x4
6: q q f2 → f1	64: \$ a u1 → q	111: \$ e x7 → b	132: b x3 q → x3
7: q q x1 → q	65: \$ a x3 → a2	f1 State	133: c x3 q → x3
8: q q x2 → f1	a2 State	112: q f1 q → f2	134: f1 x3 q → x3
9: q q x3 → q	66: q a2 b → q	113: q f1 x3 → f2	135: f2 x3 q → x3
10: q q x4 → e	67: q a2 c → q	114: \$ f1 q → a	x4 State
11: q q x5 → q	68: q a2 x1 → q	f2 State	136: q x4 q → x5
12: q q x6 → e	69: q a2 x3 → q	115: q f2 q → q	x5 State
13: q q x7 → q	70: q a2 x5 → q	116: q f2 x3 → q	137: q x5 q → x5
14: q q x8 → b	71: q a2 x7 → q	u0 State	138: a2 x5 q → x6
15: a q q → c	72: \$ a2 b → q	117: \$ u0 q → a	139: b x5 q → x5
16: a q x3 → c	73: \$ a2 c → q	u1 State	140: c x5 q → x5
17: b q q → c	74: \$ a2 x3 → q	118: a u1 q → u2	141: e x5 q → x5
18: b q x3 → c	75: \$ a2 x5 → q	u2 State	x6 State
19: b q x5 → c	76: \$ a2 x7 → q	119: q u2 q → u3	142: q x6 q → x7
20: b q x7 → c	b State	u3 State	x7 State
21: c q q → q	77: q b q → b	120: q u3 q → u4	143: q x7 q → x7
22: c q x3 → q	78: q b b → b	u4 State	144: a2 x7 q → x8
23: c q x5 → q	79: q b x3 → b	121: q u4 q → u5	145: b x7 q → x7
24: c q x7 → q	80: q b x5 → b	u5 State	146: c x7 q → x7
25: e q q → q	81: q b x7 → b	122: q u5 q → u6	147: e x7 q → x7
26: e q x5 → q	82: a2 b b → a2	u6 State	x8 State
27: e q x7 → q	83: a2 b c → a2	123: q u6 q → u7	148: q x8 q → b
28: f1 q q → q	84: a2 b x1 → a2	u7 State	
29: f1 q x3 → q	85: a2 b x3 → a2	124: q u7 q → x3	
30: f2 q q → q	86: a2 b x5 → a2	x1 State	
31: f2 q x3 → q	87: a2 b x7 → a2	125: q x1 q → x2	
32: u0 q q → u1	88: b b b → b	126: a2 x1 q → x1	
33: u1 q q → q	89: b b c → b	127: b x1 q → x1	
34: u2 q q → q	90: b b x1 → b		
35: u3 q q → q	91: b b x3 → b		
36: u4 q q → q	92: b b x5 → b		
37: u5 q q → q	93: b b x7 → b		
38: u6 q q → q	94: \$ b q → a2		
39: u7 q q → q	95: \$ b b → a2		
40: x1 q q → q	96: \$ b x5 → a2		
41: x2 q q → q	97: \$ b x7 → a2		
42: x3 q q → q	c State		
43: x4 q q → q	98: a2 c q → b		
44: x5 q q → q	99: a2 c x3 → b		
45: x6 q q → q	100: a2 c x5 → b		
46: x7 q q → q	101: a2 c x7 → b		
47: x8 q q → x1	102: b c q → c		
48: \$ q q → q	103: b c x3 → c		
49: \$ q a2 → q	104: b c x5 → c		
50: \$ q b → b	105: b c x7 → c		
51: \$ q e → e			
52: \$ q f1 → q			
53: \$ q f2 → f1			
54: \$ q u2 → q			
55: \$ q u3 → q			
56: \$ q u4 → q			
57: \$ q u5 → q			
58: \$ q u6 → q			

Table 3: A transition rule set \mathcal{R}_{n^3-1} .

q q q → q;	u1 q q → q;	u2 q q → q;
u3 q q → q;	u4 q q → q;	u5 q q → q;
u6 q q → q;	u7 q q → q;	\$ u0 q → a;
\$ a u1 → q;	\$ q u2 → q;	\$ q u3 → q;
\$ q u4 → q;	\$ q u5 → q;	\$ q u6 → q;
\$ q u7 → a;	u0 q q → u1;	a u1 q → u2;
q u2 q → u3;	q u3 q → u4;	q u4 q → u5;
q u5 q → u6;	q u6 q → u7;	q u7 q → x3;

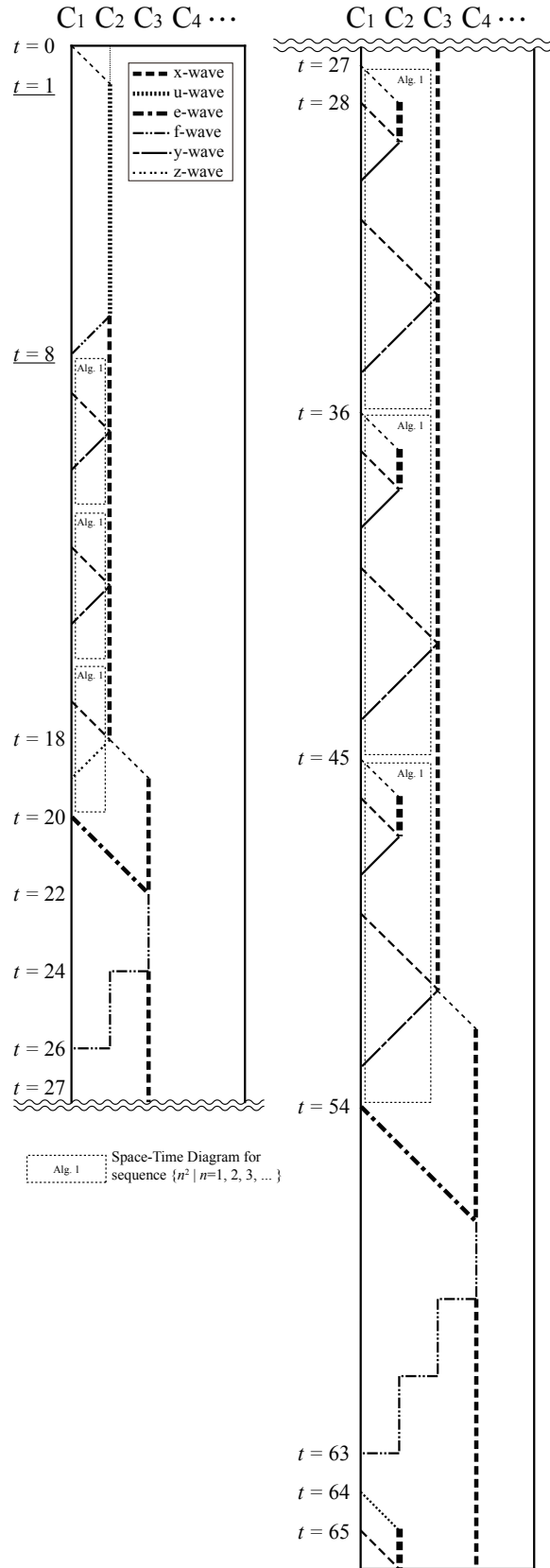


Figure 4: Space-time diagram for real-time generation of sequence $\{n^3 \mid n = 1, 2, 3, \dots\}$.

	1	2	3	4	5	6	7	8	9	10	11	12	13	14	15
0	u0	q	q	q	q	q	q	q	q	q	q	q	q	q	q
1	a	u1	q	q	q	q	q	q	q	q	q	q	q	q	q
2	q	u2	q	q	q	q	q	q	q	q	q	q	q	q	q
3	q	u3	q	q	q	q	q	q	q	q	q	q	q	q	q
4	q	u4	q	q	q	q	q	q	q	q	q	q	q	q	q
5	q	u5	q	q	q	q	q	q	q	q	q	q	q	q	q
6	q	u6	q	q	q	q	q	q	q	q	q	q	q	q	q
7	q	u7	q	q	q	q	q	q	q	q	q	q	q	q	q
8	a	x3	q	q	q	q	q	q	q	q	q	q	q	q	q

Figure 5: Configurations of sequence generator for $\{n^3 \mid n = 1, 2, 3, \dots\}$ in the space-time domain such that $C_\ell, 1 \leq \ell \leq 15, 0 \leq t \leq 8$.

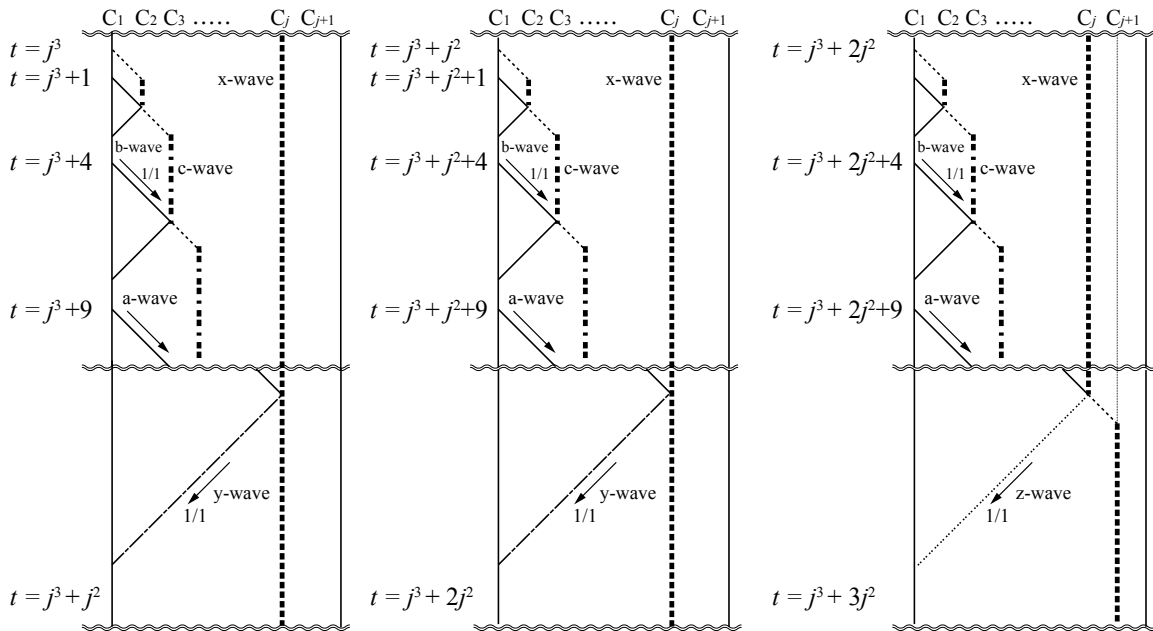


Figure 6: Space-time diagram for real-time generation of sequence $\{n^3 \mid n = 1, 2, 3, \dots\}$ when time $j^3 \leq t \leq j^3 + 3j^2$.

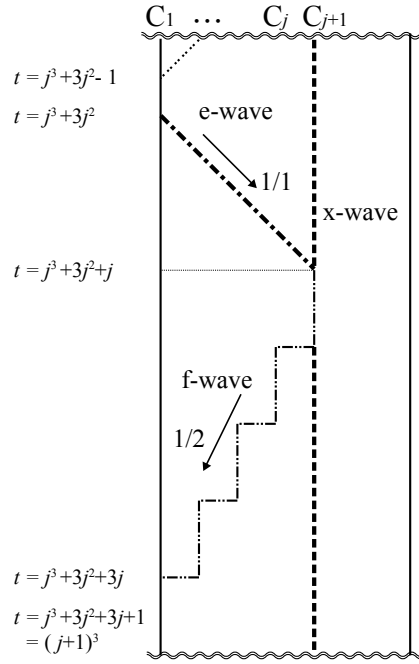


Figure 7: Space-time diagram for real-time generation of sequence $\{n^3 \mid n = 1, 2, 3, \dots\}$ when time $j^3 + 3j^2 \leq t \leq j^3 + 3j^2 + 3j + 1$.

$$t = (j + 1)^3 : \underbrace{[1]}_a \underbrace{[2, \dots, j]}_{q, \dots, q} \underbrace{[j+1]}_{x3} \underbrace{[j+2, \dots]}_{q, \dots, q}.$$

We have implemented the sequence generation algorithm for $\{n^3 \mid n = 1, 2, 3, \dots\}$ on a computer and examined the validity of the table from $t = 0$ to $t = 20000$ steps. In Figure 8, we show a number of configurations in the space-time domain such that $C_i, 1 \leq i \leq 8, 0 \leq t \leq 283$.

3.3 A implementation of real-time sequence generation algorithm for $\{n^4 \mid n = 1, 2, 3, \dots\}$

In this section, we extend the generation algorithm for $\{n^3 \mid n = 1, 2, 3, \dots\}$ shown in the previous section, present a real-time sequence generation algorithm for $\{n^4 \mid n = 1, 2, 3, \dots\}$. This algorithm contains the real-time sequence generation algorithms for $\{n^2 \mid n = 1, 2, 3, \dots\}$ and $\{n^3 \mid n = 1, 2, 3, \dots\}$ inside. Let i be a natural number such that $i \geq 1$, g_i be an infinite monotonically increasing positive integer sequence defined on natural numbers such that $g_1 = 1, g_2 = 16, g_3 = 81, \dots, g_i = i^4, h_i$ be a difference sequence of g_i such that $h_i = 4i^3 + 6i^2 + 4i + 1$.

3.3.1 Space-Time Diagram

Let M be a CA. In Figure 9, we show a space-diagram for real-time generation of sequence $\{n^4 \mid n = 1, 2, 3, \dots\}$.

Let j be a natural number such that $j \geq 2$. At time $t = j^4$, M takes as follows:

$$t = j^4 : \underbrace{[1]}_a \underbrace{[2, \dots, j-1]}_{q, \dots, q} \underbrace{[j]}_{x3} \underbrace{[j+1, \dots]}_{q, \dots, q}.$$

The communication cell C_1 takes the special state a at time $t = g_j = j^4$. At the time $t = g_j + h_j = j^4 + 4j^3 + 6j^2 + 4j + 1 = (j + 1)^4$, the communication cell C_1 falls into the special state a by waves

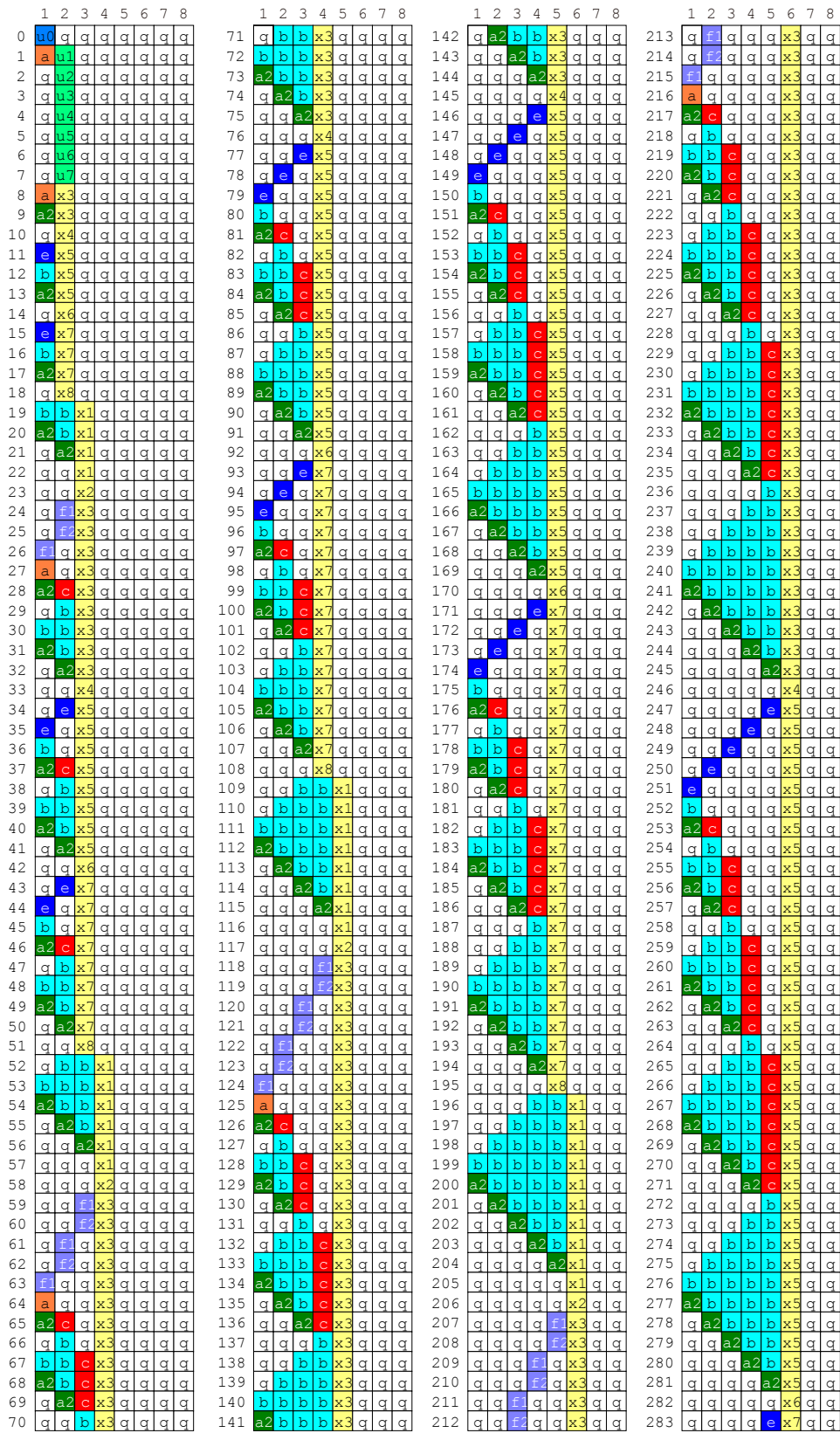


Figure 8: Some configurations of real-time generation of sequence $\{n^3 \mid n = 1, 2, 3, \dots\}$.

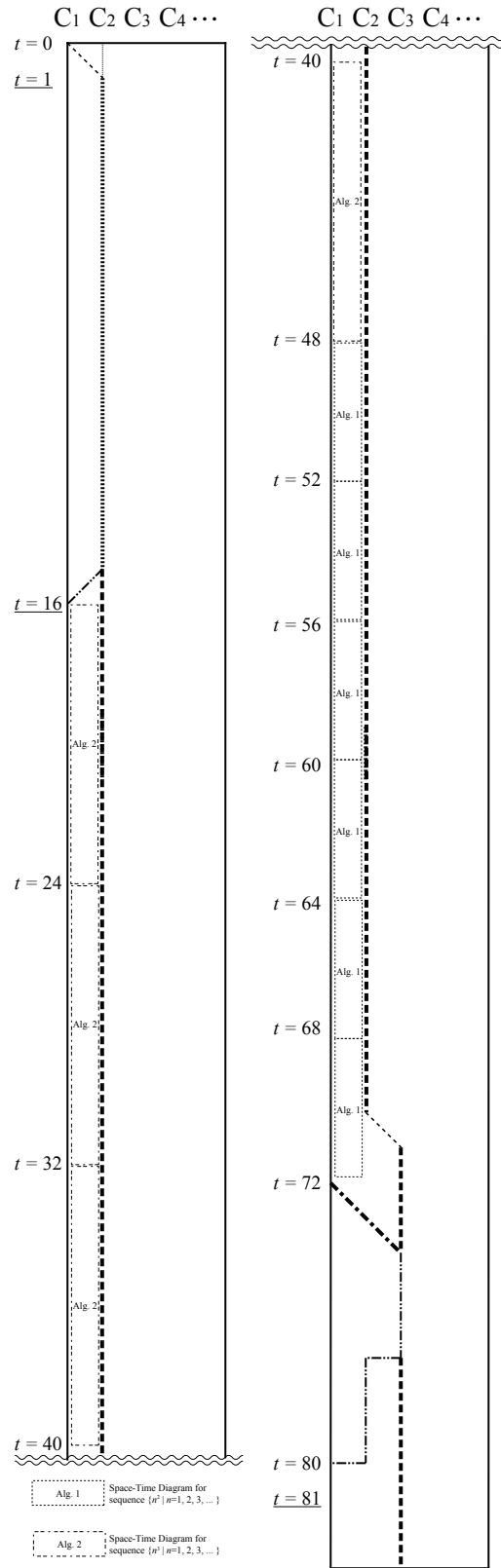


Figure 9: Space-time diagram for real-time generation of sequence $\{n^4 \mid n = 1, 2, 3, \dots\}$.

propagation according to the each term in the difference sequence of $h_j = 4j^3 + 6j^2 + 4j + 1$. We consider the generation process when $j^4 \leq t \leq j^4 + 4j^3$, $j^4 + 4j^3 \leq t \leq j^4 + 4j^3 + 6j^2$ and $j^4 + 4j^3 + 6j^2 \leq t \leq j^4 + 4j^3 + 6j^2 + 4j + 1$, respectively.

Case (I) $j^4 \leq t \leq j^4 + 4j^3$: At first, the sequence generation algorithm for $\{n^3 | n = 1, 2, 3, \dots\}$ works four times between the leftmost cell C_1 and the x-wave. After the generation algorithm for $\{n^3 | n = 1, 2, 3, \dots\}$ finishes four times, the next generation process is started at time $t = j^4 + 4j^3$.

Case (II) $j^4 + 4j^3 \leq t \leq j^4 + 4j^3 + 6j^2$: Next, the sequence generation algorithm for $\{n^2 | n = 1, 2, 3, \dots\}$ works six times between the leftmost cell C_1 and the x-wave. After the generation algorithm for $\{n^2 | n = 1, 2, 3, \dots\}$ finishes six times, the next generation process is started at time $t = j^4 + 4j^3 + 6j^2$.

Case (III) $j^4 + 4j^3 + 6j^2 \leq t \leq j^4 + 4j^3 + 6j^2 + 4j + 1$: In this case, the e-, f- and z-waves propagate for space-time diagram shown in Figure 10.

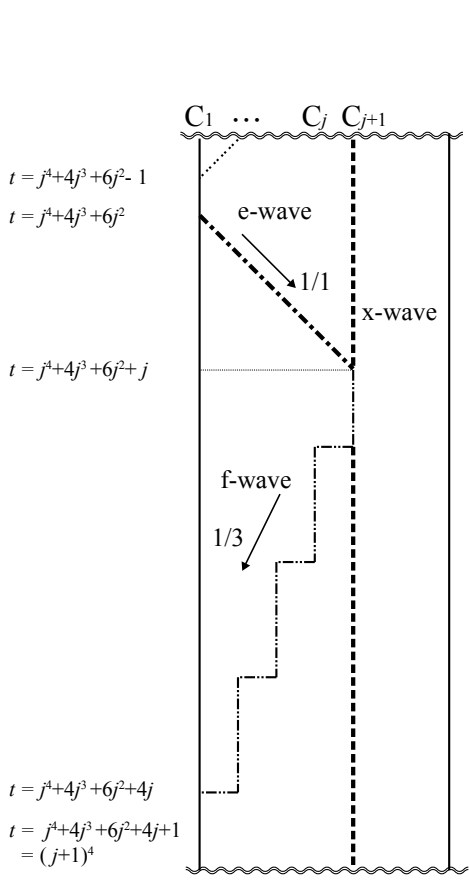


Figure 10: Space-time diagram for real-time generation of sequence $\{n^4 | n = 1, 2, 3, \dots\}$ when time $j^4 + 4j^3 + 6j^2 \leq t \leq j^4 + 4j^3 + 6j^2 + 4j + 1$.

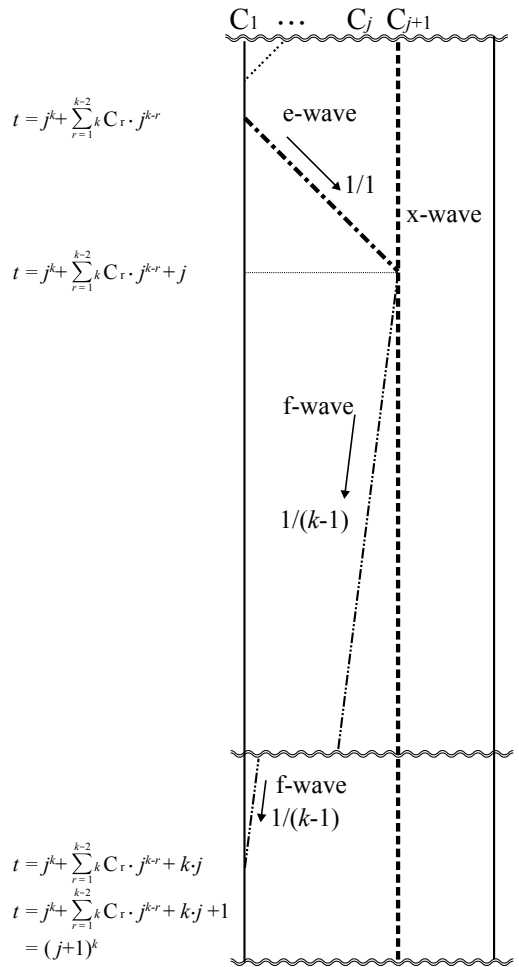


Figure 11: Space-time diagram for real-time generation of sequence $\{n^k | n = 1, 2, 3, \dots\}$ when time $j^k \leq t \leq j^k + \sum_{r=1}^{k-2} kC_r \cdot j^{k-r}$.

In the case of the generation algorithm for $\{n^4 | n = 1, 2, 3, \dots\}$, the f-wave propagate to the left direction at $1/3$ speed. At time $t = j^4 + 4j^3 + 6j^2$, the e-wave is generated, and propagates

in right direction at $1/1$ speed. The e-wave collides with the x-wave on the cell C_{j+1} at time $t = j^4 + 4j^3 + 6j^2 + j$. Then the e-wave is deleted and the f-wave is generated. The f-wave propagates in left direction at $1/3$ speed and hits the leftmost cell C_1 at time $t = j^4 + 4j^3 + 6j^2 + 4j$. So, the f-wave is eliminated. At the next step $t = j^4 + 4j^3 + 6j^2 + 4j + 1 = (j+1)^4$, the communication cell C_1 falls into the special state **a**. Then M takes as follows:

$$t = (j+1)^4 : \underbrace{\text{a}}^{[1]} \underbrace{\text{q}, \dots, \text{q}}^{[2, \dots, j]} \underbrace{\text{x3}}^{[j+1]} \underbrace{\text{q}, \dots, \text{q}}^{[j+2, \dots]}$$

We have implemented the sequence generation algorithm for $\{n^4 | n = 1, 2, 3, \dots\}$ on a computer and examined the validity of the table from $t = 0$ to $t = 20000$ steps.

3.4 A realization of real-time sequence generation algorithm for $\{n^k | n = 1, 2, 3, \dots\}$

In this section, we extend and generalize generation algorithms for $\{n^2 | n = 1, 2, 3, \dots\}$, $\{n^3 | n = 1, 2, 3, \dots\}$ and $\{n^4 | n = 1, 2, 3, \dots\}$, show that sequence $\{n^k | n = 1, 2, 3, \dots\}$ can be generated in real-time. Let i be a natural number such that $i \geq 1$, p_i be an infinite monotonically increasing positive integer sequence defined on natural numbers such that $p_i = i^k$, s_i be a difference sequence of p_i such that $s_i = (i+1)^k - i^k = \sum_{r=0}^{k-1} {}_k C_r \cdot i^{k-r} - i^k = \sum_{r=1}^{k-1} {}_k C_r \cdot i^{k-r} + k \cdot i + 1$. Let M be a CA, j be a natural number such that $j \geq 2$. At time $t = j^k$, M takes as follows:

$$t = j^k : \underbrace{\text{a}}^{[1]} \underbrace{\text{q}, \dots, \text{q}}^{[2, \dots, j-1]} \underbrace{\text{x3}}^{[j]} \underbrace{\text{q}, \dots, \text{q}}^{[j+1, \dots]}$$

The communication cell C_1 takes the special state **a** at time $t = p_j = j^k$. At the time $t = p_j + s_j = j^k + \sum_{r=1}^{k-2} {}_k C_r \cdot j^{k-r} + k \cdot j + 1 = (j+1)^k$, the communication cell C_1 falls into the special state **a** by waves propagation according to the each term in the difference sequence of $s_j = \sum_{r=1}^{k-2} {}_k C_r \cdot j^{k-r} + k \cdot j + 1$. We consider the generation process when $j^k \leq t \leq j^k + \sum_{r=1}^{k-2} {}_k C_r \cdot j^{k-r}$ and $j^k + \sum_{r=1}^{k-2} {}_k C_r \cdot j^{k-r} \leq t \leq j^k + \sum_{r=1}^{k-2} {}_k C_r \cdot j^{k-r} + k \cdot j + 1$, respectively.

Case (I) $j^k \leq t \leq j^k + \sum_{r=1}^{k-2} {}_k C_r \cdot j^{k-r}$: Let ℓ be natural number such that $1 \leq \ell \leq k-2$.

In this case, generation algorithms for $\{n^2 | n = 1, 2, 3, \dots\}$, $\{n^3 | n = 1, 2, 3, \dots\}$, \dots , $\{n^\ell | n = 1, 2, 3, \dots\}$ and $\{n^{\ell+1} | n = 1, 2, 3, \dots\}$ work ${}_k C_{k-1-\ell}$ times between the leftmost cell C_1 and the x-wave, respectively. After the generation algorithms for $\{n^2 | n = 1, 2, 3, \dots\}$, $\{n^3 | n = 1, 2, 3, \dots\}$, \dots , $\{n^{k-2} | n = 1, 2, 3, \dots\}$ and $\{n^{k-1} | n = 1, 2, 3, \dots\}$ finish, the next generation process is started at time $t = j^k + \sum_{r=1}^{k-2} {}_k C_r \cdot j^{k-r}$.

Case (II) $j^k + \sum_{r=1}^{k-2} {}_k C_r \cdot j^{k-r} \leq t \leq j^k + \sum_{r=1}^{k-2} {}_k C_r \cdot j^{k-r} + k \cdot j + 1$: In this case, the e-, f- and z-waves propagate for space-time diagram shown in Figure 11.

In this case, the f-wave propagate to the left direction at $1/(k-1)$ speed. At time $t = j^k + \sum_{r=1}^{k-2} {}_k C_r \cdot j^{k-r}$, the e-wave is generated, and propagates in right direction at $1/1$ speed. The e-wave collides with the x-wave on the cell C_{j+1} at time $t = j^k + \sum_{r=1}^{k-2} {}_k C_r \cdot j^{k-r} + j$. Then the e-wave is deleted and the f-wave is generated. The f-wave propagates in left direction at $1/(k-1)$ speed and hits the leftmost cell C_1 at time $t = j^k + \sum_{r=1}^{k-2} {}_k C_r \cdot j^{k-r} + k \cdot j$. So, the f-wave is eliminated. At the next step $t = j^k + \sum_{r=1}^{k-2} {}_k C_r \cdot j^{k-r} + k \cdot j + 1 = (j+1)^k$, the communication cell C_1 falls into the special state **a**. Then M takes as follows:

$$t = (j+1)^k : \underbrace{\text{a}}^{[1]} \underbrace{\text{q}, \dots, \text{q}}^{[2, \dots, j]} \underbrace{\text{x3}}^{[j+1]} \underbrace{\text{q}, \dots, \text{q}}^{[j+2, \dots]}$$

Thus, sequence $\{n^k | n = 1, 2, 3, \dots\}$ can be generated in real-time for any k by one-dimensional CA.

Next, we consider about the number of internal states to realize generation of sequence $\{n^k \mid n = 1, 2, 3, \dots\}$ in real-time on the CA. A real-time sequence generator for $\{n^k \mid n = 1, 2, 3, \dots\}$ consists of a semi-infinite array of finite state automaton $M = (Q_k, \delta, \mathbf{n0}, \mathbf{a})$. Let $P_{1,k}, P_{2,k}, P_{3,k}$ be a finite set of internal states which are subset of Q_k . From Section 3.1, $|Q_2| = 4$. When $k \geq 3$, $Q_k \setminus Q_{k-1} = P_{1,k} \cup P_{2,k} \cup P_{3,k}$. Internal state sets $P_{1,k}, P_{2,k}$ and $P_{3,k}$ are as follows:

- $P_{1,k}$: Internal state set used for the generation process at time $0 \leq t \leq 2^k$
A internal state set $\{\mathbf{u0}, \mathbf{u1}, \mathbf{u2}, \dots, \mathbf{u}2^k - 1\}$ is used for the generation processes at time $0 \leq t \leq 2^k$. Thus, $|P_{1,k}| = 2^k$.
- $P_{2,k}$: Internal state set representing e- and f-waves
The e-wave is represented by the state \mathbf{e} , and the f-wave is represented by state $\mathbf{f1}, \mathbf{f2}, \mathbf{f3}, \dots, \mathbf{fk} - 1$. Therefore, $P_{2,k} = \{\mathbf{e}, \mathbf{f1}, \mathbf{f2}, \mathbf{f3}, \dots, \mathbf{fk} - 1\}$, and $|P_{2,k}| = k$.
- $P_{3,k}$: Internal state set representing the x-wave
The x-wave exists in the rightmost cell whose state is not a quiescent state \mathbf{q} . $P_{3,k}$ is determined by $P_{3,k-1}, P_{3,k-2}, P_{3,k-3}, \dots, P_{3,2}$ and number of repetitions of generation algorithm for $\{n^{k-1} \mid n = 1, 2, 3, \dots\}, \{n^{k-2} \mid n = 1, 2, 3, \dots\}, \dots, \{n^2 \mid n = 1, 2, 3, \dots\}$. However, the c-wave operates as the x-wave, when $k = 2$. Therefore, $|P_{3,k}| = 2 + \sum_{r=1}^{k-2} {}_k C_r \cdot |P_{3,k-r} + 1|$, $|P_{3,2}| = 1$.

From the above, the number of internal states $|Q_k|$ of sequence generator for $\{n^k \mid n = 1, 2, 3, \dots\}$ is expressed as follows:

$$|Q_k| = \begin{cases} 4 & k = 2 \\ |Q_{k-1}| + 2^k + k + |P_{3,k}| & k \geq 3, \end{cases}$$

$$|P_{3,k}| = \begin{cases} 1 & k = 2 \\ 2 + \sum_{r=1}^{k-2} {}_k C_r \cdot |P_{3,k-r} + 1| & k \geq 3. \end{cases}$$

4 Conclusion

A sequence generation problem on CAs has been studied. It has been shown that sequence $\{n^k \mid n = 1, 2, 3, \dots\}$ can be generated in real-time by a one-dimensional CA. Our sequence generation algorithms would be useful in the simulation and modeling biological pattern formations using CAs. A further improvement on the proof of the correctness of the algorithm, the number of states and its lower bound would be interesting.

References

- [1] M. Arisawa, "On the generation of integer series by the one-dimensional iterative arrays of finite state machines", The Trans. of IECE, vol. 54-C, no.8, pp.759-766, 1971 (in Japanese).
- [2] P. C. Fischer, "Generation of primes by a one-dimensional real-time iterative array", J. of ACM, vol.12, no.3, pp.388-394, 1965.
- [3] N. Kamikawa and H. Umeo, "Some algorithms for real-time generation of non-regular sequences on one-bit inter-cell-communication cellular automata", Proc. of SICE Annual Conference 2007, pp.953-958, 2007.
- [4] N. Kamikawa and H. Umeo, "Some state-efficient algorithms for real-time generation of non-regular sequences on cellular automata", Proc. of the 13th International Symposium on Artificial Life and Robotics, pp.47-50, 2008.

- [5] N. Kamikawa and H. Umeo, "A design of algorithms for real-time generation of linear-recursive sequences on cellular automata", Proc. of the 14th International Symposium on Artificial Life and Robotics, pp.281–286, 2009.
- [6] N. Kamikawa and H. Umeo, "A study on sequence generation powers of small cellular automata", SICE Journal of Control, Measurement, and System Integration, vol. 5, no. 4, pp. 191–199, DOI: 10.9746/jcmsi.5.191, 2012.
- [7] N. Kamikawa and H. Umeo, "A construction of five-state real-time Fibonacci sequence generator", Artificial Life and Robotics, vol. 21, no. 4, pp. 531–539, DOI: 10.1007/s10015-016-0309-2, 2016.
- [8] N. Kamikawa and H. Umeo, "Two Implementations of Real-Time Sequence Generator for $\{n^3 | n = 1, 2, 3, \dots\}$ and Their Comparison", International Journal of Networking and Computing – www.ijnc.org", ISSN 2185-2847 Vol. 9, No. 2, pp. 257-275, 2019.
- [9] N. Kamikawa and H. Umeo, "A Construction of Real-Time Sequence Generation Algorithm for $\{n^4 | n = 1, 2, 3, \dots\}$ ", 11th International Workshop on Parallel and Distributed Algorithms and Applications, pp.215-220, 2019.
- [10] I. Korec, "Real-time generation of primes by a one-dimensional cellular automaton with 9 states", Proc. of the 2nd International Colloquium on Universal Machines and Computations, pp.101–116, 1998.
- [11] J. von Neumann, "Theory of self-reproducing automata", A. W. Burks (Ed.), p. 388, Univ. of Illinois Press, 1968.